

Cite this: *Green Chem.*, 2012, **14**, 2899

www.rsc.org/greenchem

PAPER

A new route of CO₂ catalytic activation: syntheses of *N*-substituted carbamates from dialkyl carbonates and polyureas†

Jianpeng Shang,^{a,b} Shimin Liu,^{a,b} Xiangyuan Ma,^a Liujin Lu^a and Youquan Deng^{*a}

Received 25th April 2012, Accepted 7th August 2012

DOI: 10.1039/c2gc36043h

This paper reports an effective route for the syntheses of *N*-substituted dicarbamates from dialkyl carbonates and polyurea derivatives, in which polyurea derivatives could be successfully synthesized from aliphatic diamines and CO₂ in the absence of any catalyst. Under the optimized reaction conditions, various *N*-substituted carbamates were successfully synthesized with 93–98% isolated yields over a MgO–ZnO catalyst. The catalyst could be reused for several runs without deactivation. The catalysts were characterized with X-ray photoelectron spectroscopy, X-ray diffraction and temperature-programmed desorption.

1. Introduction

The reduction, capture, or utilization of CO₂ discharged from industrial processes is one of the greatest scientific and technological challenges of the 21st century.¹ Moreover, CO₂ is a non-toxic, abundant and economical C1 feed stock and various methodologies have been developed for chemical fixation of CO₂ to valuable chemicals, including urea, salicylic acid, synthesis gas, carbonates and urea derivatives.^{2–7} Among them, urea derivatives are widely used as intermediates for biologically active compounds, pesticides, herbicides, medicines, and pigments.^{8–10} Meanwhile, they can also be regarded as potential precursors of carbamates and isocyanates, which are useful raw materials of polyurethanes.¹¹ In this regard, successful routes to urea derivatives directly from CO₂ and amines have been reported. Although the 1,3-disubstituted ureas and cyclic ureas are obtained in moderate to excellent yields from monoamine^{7,12–14} and ethylene diamine,¹⁵ respectively, there were limited reports for the polyurea derivatives syntheses directly from CO₂ and diamines.¹⁶ Moreover, organic carbonates are also important intermediates for organic synthesis, in which they are mainly used as alkylating agents, carbonylating agents, and as a substitute for phosgene in the syntheses of polycarbonates and polyurethanes.^{17–20}

N-substituted carbamates represent an important class of compounds showing various interesting properties and have wide utility in various areas, including pharmaceuticals, agrochemicals, protection of amino groups in peptide chemistry, and as

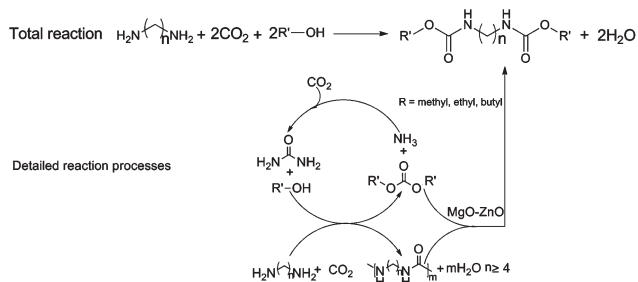
linkers in combinational chemistry.^{21–23} Moreover, they have become the potential raw material for the non-phosgene syntheses of isocyanates through thermal decomposition,^{24–26} such as 1,6-hexamethylene diisocyanate, isophorone diisocyanate, 4,4'-dicyclohexylmethane diisocyanate and 4,4'-diphenylmethane diisocyanate. The commercial process for carbamates syntheses has been almost exclusively based on the phosgene technology,^{27,28} however, this process uses highly toxic phosgene and produces highly corrosive hydrochloride as a side product. Thus, great efforts have been made to explore environmentally benign methods for carbamates production. There are several green alternative routes for carbamates syntheses, such as reductive carbonylation of nitro compounds,^{29,30} oxidative carbonylation of amines,^{31,32} methoxycarbonylation of amines^{33,34} and alcoholysis of substituted ureas.^{35,36} However, the later two reactions result in a poor atom economy and in each case alcohol or amine are produced as byproducts, which decrease the efficiency of the functional groups of the reagents. To improve the atom economy, those two reactions have been coupled to synthesize the *N*-substituted carbamates, *i.e.*, *N*-substituted carbamates have been synthesized by using urea derivatives and dialkyl carbonates as raw materials. Till now, several catalysts, including silica gel, Bu₂SnO, NaOCH₃, PbCO₃ and La/SiO₂, have been extensively studied for the *N*-substituted monocarbamate syntheses.^{37–41} However, there was no report for *N*-substituted dicarbamate syntheses from dialkyl carbonates and polyurea derivatives. Another promising approach is the direct syntheses of carbamates from CO₂, amines and alcohols, however, only monocarbamates could be synthesized with ≤66% to >90% of isolated yields.^{42–44} Moreover, the direct *N*-substituted dicarbamates syntheses from CO₂, diamines and alcohols was not reported.

Herein, we report an effective route for the syntheses of polyurea derivatives from diamines and CO₂ in the absence of any catalyst, which are then reacted with dialkyl carbonates to synthesize *N*-substituted dicarbamates over a MgO–ZnO catalyst, Scheme 1. Since the polyurea derivatives and dialkyl carbonates

^aCentre for Green Chemistry and Catalysis, Lanzhou Institute of Chemical Physics, Chinese Academy of Sciences, 730000 Lanzhou, China. E-mail: ydeng@licp.cas.cn; Fax: +86-931-4968116; Tel: +86-931-4968116

^bGraduate School of the Chinese Academy of Sciences, 100039 Beijing, China

†Electronic supplementary information (ESI) available. See DOI: 10.1039/c2gc36043h



Scheme 1 Syntheses of *N*-substituted dicarbamates from dialkyl carbonates and polyurea derivatives based on diamines and CO_2 .

could be successfully synthesized from CO_2 , such a process not only improves the functional group efficiency of the reagents, but also fulfills the optimum utilization of CO_2 .

2. Experimental

2.1 Polyurea derivatives syntheses from diamines and CO_2

All reactions were carried out in a 50 mL stainless steel autoclave with a magnetic stirrer. As an example, 10 mmol of 1,6-hexamethylenediamine (HDA) and 3 mL of *N*-methyl-2-pyrrolidone (NMP) were charged in the reactor, and the reactor was saturated with CO_2 under a pressure of 2–5 MPa at room temperature. The reaction proceeded at 150–200 °C for 8–24 h. After the reaction, the autoclave was cooled down to room temperature and carefully depressurized. After water addition and filtration the resulted solid product was washed with deionized water, recovered by filtration and then thoroughly dried in vacuum. The solid product was weighed to determine the isolated yields. The filtrate was analyzed by GC (Agilent 7890) equipped with a FID detector to determine the conversion of diamine. The CP/MAS ^{13}C NMR spectra were recorded on a Bruker AVANCE II WB 400 spectrometer equipped with a 4 mm standard bore CP/MAS probehead. Fourier-transform infrared (FT-IR) spectra of solid samples were recorded at room temperature with a Bruker Vertex Nicolet 5700 FT-IR spectrometer in the region of 4000–400 cm^{-1} with a resolution of 4 cm^{-1} . X-ray diffraction (XRD) measurements were carried out on a Siemens D/max-RB powder X-ray diffractometer. The samples were scanned over the 2θ range 10–70°. Differential scanning calorimetry (DSC) experiments were carried out on a Mettler-Toledo DSC822e calorimeter with heating and cooling-rates of 10 °C min^{-1} from 0 °C up to 300 °C under N_2 flow. The first heating run was used to remove all effects due to the thermal history of the sample and only second heating runs were used.

2.2 *N*-substituted carbamates syntheses from polyurea derivatives and dialkyl carbonates

All reactions were carried out in a 90 mL stainless steel autoclave with a glass tube inside and with a magnetic stirrer. Typically, 5 mmol polyurea, 10–75 mmol dibutyl carbonate (DBC), and 3–15 wt% catalyst (based on the mass of charged polyurea) were charged successively into the autoclave. Under a nitrogen atmosphere, the reaction proceeded at 180–220 °C for 3–24 h.

After reaction, the autoclave was cooled down to room temperature. The catalyst and the unconverted polyurea were separated by filtration and then thoroughly dried in vacuum. The resulted solids were weighed and the mass of catalyst subtracted to determine the conversion of the polyurea. The qualitative and quantitative analyses of the filtrate were conducted with GC-MS (Agilent 6890/5973) and GC (Agilent 7890) equipped with a FID detector. The products were also characterized with ^1H , ^{13}C NMR and mass spectrometry.

2.3 Catalysts preparation and characterization

A series of catalysts of MgO–ZnO composite oxides with different compositions were prepared by a co-precipitation method using $\text{Mg}(\text{NO}_3)_2 \cdot 6\text{H}_2\text{O}$ and $\text{Zn}(\text{NO}_3)_2 \cdot 6\text{H}_2\text{O}$ as starting materials and Na_2CO_3 as precipitant. At room temperature, an aqueous solution containing 0–40 mmol $\text{Mg}(\text{NO}_3)_2 \cdot 6\text{H}_2\text{O}$ and 0–40 mmol $\text{Zn}(\text{NO}_3)_2 \cdot 6\text{H}_2\text{O}$ was added dropwise into 100 mL Na_2CO_3 solution (1.89 mol L^{-1}) with vigorous stirring. After filtration and washing with 300 mL distilled water, the resulted precipitates were dried at 100 °C for 12 h. Then precursors were calcined at 500 °C for 5 h. The obtained MgO–ZnO composite oxides with different compositions were denoted as MgO, 3MgO–ZnO, MgO–ZnO, MgO–3ZnO and ZnO.

The BET surface areas, pore volumes and average pore diameters of the catalysts were obtained with physisorption of N_2 using a Micromeritics ASAP 2010.

X-ray photoelectron spectroscopy (XPS) analysis were measured using a K-Alpha-surface analysis instrument with Al $\text{K}\alpha$ radiation (1361 eV) and all the binding energies were referenced to the adventitious C 1s at 285 eV.

X-ray diffraction (XRD) measurements were carried out on a Siemens D/max-RB powder X-ray diffractometer. Diffraction patterns were recorded with Cu $\text{K}\alpha$ radiation (40 mA, 40 kV) over the 2θ range 15–85°.

Temperature-programmed desorption (TPD) of CO_2 and NH_3 was carried out on a TPD flow system equipped with an MS detector (DM300, AMETEK, USA) to study the acid–base properties of the catalysts. In a typical experiment, the solid sample (100 mg with particle size 160–200 μm) was pretreated at 500 °C for 1 h under nitrogen flow (50 mL min^{-1}) and then cooled to room temperature. The sample was subsequently exposed to CO_2 (NH_3) stream (50 mL min^{-1}) at room temperature for 1 h and flushed again with nitrogen for 1 h to remove any physico-adsorbed CO_2 (NH_3). The desorption profile was recorded at a heating rate of 10 °C min^{-1} from room temperature to 500 °C.

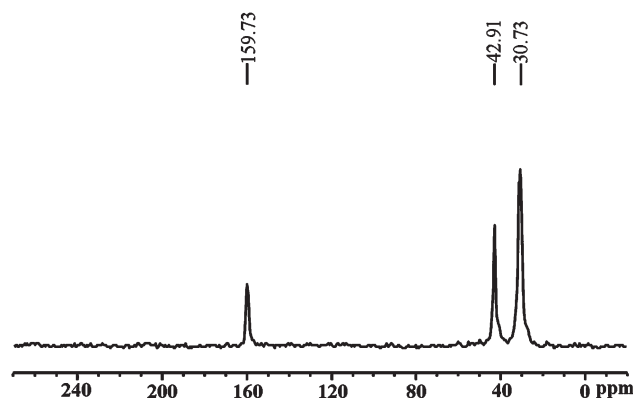
3. Results and discussions

3.1 Polyurea derivatives syntheses from diamines and CO_2

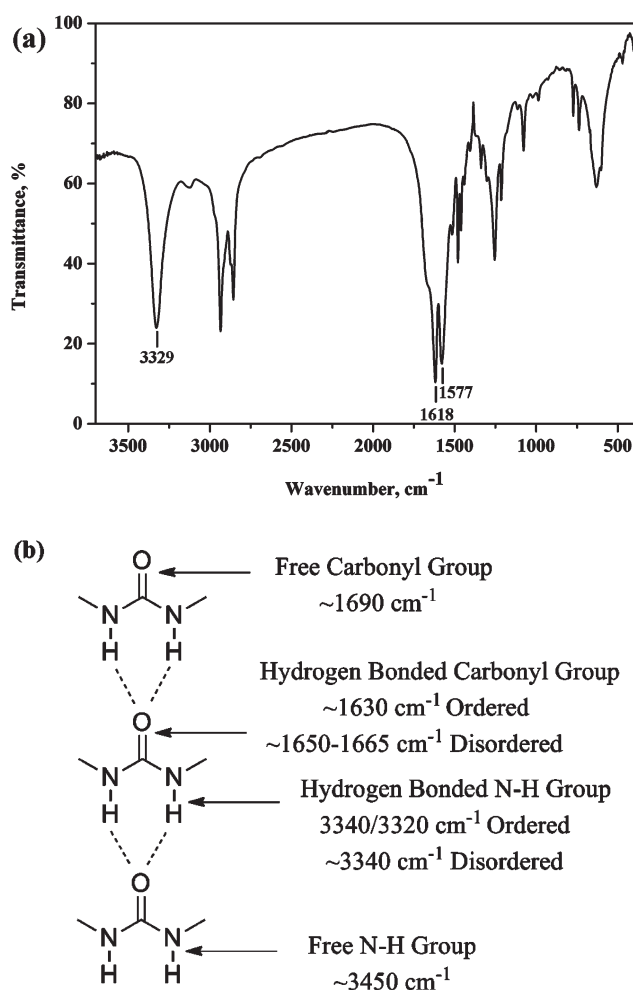
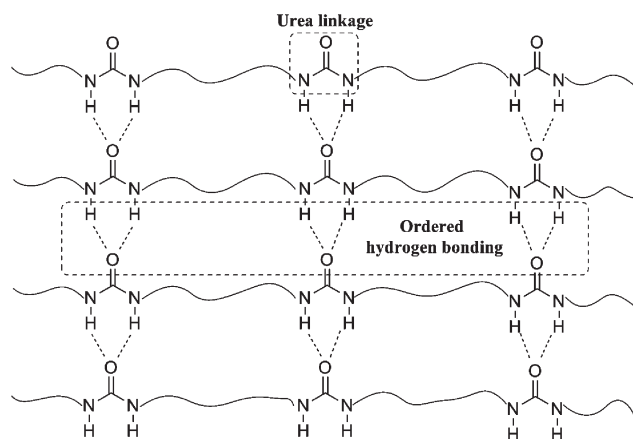
In the preliminary study, HDA was selected as a model substrate to test this protocol. The CP/MAS ^{13}C NMR spectrum of the solid product, which was produced from the reaction of HDA and CO_2 in the absence of catalyst (entry 1, Table 1), showed a characterization peak at 159.7 ppm, indicating that the formation of carbonyl in the urea linkage (Fig. 1).

Table 1 Optimization of the reaction conditions for the polyurea-HDA synthesis from CO₂ and HDA^a

Entry	Temperature (°C)	Pressure (MPa)	Time (h)	Solvent	Yield ^b (%)
1	180	4.5	24	NMP	96
2	150	4.5	24	NMP	58
3	160	4.5	24	NMP	73
4	170	4.5	24	NMP	85
5	200	4.5	24	NMP	89
6	180	4.5	8	NMP	50
7	180	4.5	12	NMP	74
8	180	4.5	16	NMP	84
9	180	4.5	20	NMP	90
10	180	2	24	NMP	20
11	180	3	24	NMP	59
12	180	5	24	NMP	97
13	180	4.5	24	None	3
14	180	4.5	24	CH ₃ CN	78
15	180	4.5	24	DMF	42
16	180	4.5	24	<i>n</i> -Decane	2
17	180	4.5	24	Butanol	62

^a Reaction conditions: 10 mmol HDA, 3 mL NMP, 50 mL autoclave.^b Isolated yield based on charged HDA.**Fig. 1** CP/MAS ¹³C NMR spectrum of the solid product of the reaction of HDA with CO₂.

Furthermore, the structure of the solid product was also characterized by FT-IR spectroscopic analyses (Fig. 2). The peaks at 1618 and 1577 cm⁻¹ are assigned to the amide I (C=O) and amide II (CO-N-H), respectively, indicating the formation of the urea linkage.^{16,45,46} Moreover, the stretching vibration of C=O and N-H were observed at 1618 and 3329 cm⁻¹, respectively, suggesting that the solid product was connected by ordered H bonding, as shown in Fig. 2, which was formed through the active H atoms of the two urea donor groups (N-H) in one urea molecule and an acceptor oxygen of the carbonyl group (C=O) in another urea molecule, but not the free urea (~1690 cm⁻¹) or disordered H bonding (~1650–1665 cm⁻¹).^{45,46} From those two results, it could be conjectured that the solid product based on HDA and CO₂ has the polyurea structure with the urea linkage and connected by

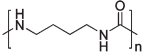
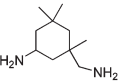
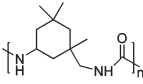
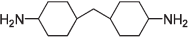
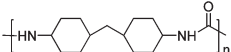
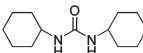
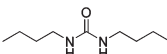
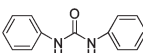
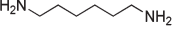
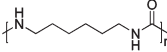
**Fig. 2** (a) The FT-IR spectrum of the solid product of the reaction of HDA with CO₂. (b) Band assignments for the polyurea carbonyl and N-H stretching modes.⁴⁶**Fig. 3** The network structure of the polyurea-HDA.

the ordered H bonding, as schematically shown in the Fig. 3. Therefore, the polyurea derivative (denoted as polyurea-HDA) could be successfully produced from the reaction of HDA and CO₂ in the absence of catalyst.

In order to select the optimum reaction conditions, experiments focused on the effects of the reaction temperature, time, CO₂ pressure and solvent. The main results are presented in Table 1. The polyurea-HDA yield increased rapidly with increasing the reaction temperature and the yield reached a maximum at 180 °C, *i.e.* 96% (entries 1–4). Whereas, further increase of the reaction temperature up to 200 °C caused a decrease in the yield, presumably because that it was a reversible and exothermic reaction, and was shifted to the left with increasing the temperature (entry 5).⁴⁷ By increasing the reaction times, the yield of polyurea-HDA increased smoothly and reached a maximum yield after 24 h (entries 6–9). We also found that the polyurea-HDA yield was sensitive to the CO₂ pressure (entries 10–12). The yield of polyurea-HDA increased with increasing the pressure up to 5 MPa, but the yield was more sensitive to pressure up to 4.5 MPa, and the effect of pressure on the yield was much smaller at the higher pressure. The main reason is that at lower pressure, an increase in pressure enhances the reaction rate because CO₂ is a reactant and the solubility of CO₂ in the reaction phase increased with increasing CO₂ pressure. When the pressure is higher than 4.5 MPa, the concentration of CO₂ in the reaction phase is high enough, and therefore, the effect of pressure on the yield is very limited at the higher pressure. Moreover, the solvent played an important role for such reactions (entries 13–16). There was nearly no product formed without the addition of any solvent, suggesting that the solvent is necessary for this reaction to proceed well. The reaction in a polar solvent, such as NMP, CH₃CN and dimethyl formamide (DMF), resulted in a higher yield of polyurea-HDA than in an apolar solvent, such as *n*-decane. Of those, the highest yield of polyurea-HDA was achieved when NMP was used as the solvent. Other amides like DMF were tested as well, and important side product formation was observed because DMF is not inert in the reaction conditions. When another basic solvent like acetonitrile was used, however, the result was far inferior to those obtained in NMP. All these results suggested that both the basicity and polarity of the solvent have great effects on the reaction. Additionally, in order to investigate the possibility of the one-pot reaction of diamine, CO₂ and alcohol to afford the corresponding *N*-substituted carbamate, butanol was used as a solvent for the reaction of HDA and CO₂, entry 17. The results showed that the corresponding carbamate was not detected and the main product was the polyurea-HDA, which indicated that the one-pot reaction of diamines, CO₂ and alcohol to the corresponding dicarbamates was unfeasible under the present conditions.

In order to investigate the limitations and scope of this protocol, the reaction between several different diamines and monoamines, such as 1,4 butanediamine (BDA), isophorone diamine (IPDA), 4,4'-diaminodicyclohexyl methane (HMDA), cyclohexylamine (CA), butylamine (BA) and aniline with CO₂ for the corresponding polyurea and urea derivatives were further tested in the optimized conditions, and the results are given in Table 2. The solid products obtained from other diamines (entries 1–3) with CO₂ were also analyzed with CP/MAS ¹³C NMR and FT-IR, and the results are shown in Fig. S1 and S2,[†] respectively. All the CP/MAS ¹³C NMR spectra showed a specific peak around 160.0 ppm, indicating the formation of the carbonyl in the urea linkage (Fig. S1[†]). The results of FT-IR showed that the solid products obtained from BDA and HMDA with CO₂ gave

Table 2 Syntheses of polyurea and urea derivatives with different diamines and amines^a

Entry	Amines	Product	Yield ^b (%)
1			78
2			93
3			94
4			40
5			34
6			No reaction
7			94 ^c

^a Reaction conditions: 10 mmol diamine or amine, 3 mL NMP, 4.5 MPa CO₂, 180 °C, 24 h, 50 mL autoclave. ^b Isolated yield based on charged amine. ^c 5 mmol HDA were charged.

similar FT-IR spectra with the polyurea-HDA, but for the solid product obtained from IPDA and CO₂, the stretching vibrations of C=O and N–H were observed at 1648 and 3340 cm⁻¹ (Fig. S2[†]), respectively, suggesting that the disordered H bonding may be formed as shown in Fig. 2, which could be ascribed to the lower regularity of the cyclic structure with a side chain substituent. All those results suggested that the polyurea derivatives were successfully formed from the diamines and CO₂. The yields of the corresponding polyurea of aliphatic diamines were much higher than that of monoamines (entries 4–5). This may be due to the fact that the binding of CO₂ by an amine requires two equivalents of an amine, where one acts as a base while the other binds the CO₂: (2 R–NH₂ + CO₂ → R–NH₃⁺ + R–NH–CO₂⁻ or 2 NH₂–R–NH₂ + CO₂ → 2⁺NH₃–R–NH–CO₂⁻ or NH₂–R–NH–CO₂⁻ + NH₂–R–NH₃⁺), and such an intermediate process may be more favourable for a diamine than a monoamine. However, aniline was found to be unreactive, and only starting material was recovered (entry 6). This could be ascribed to the weaker basicity of the aromatic amine. Moreover, in order to investigate the reactivity of diamine and monoamine with the same amounts of NH₂ groups, the reaction of CO₂ with 5 mmol HDA was further tested, which has the same amount of the NH₂ groups as 10 mmol monoamine. The result was added in Table 2 entry 7 and showed that the yield of polyurea-HDA was 94%, which was also higher than that of monoamine, suggesting that the higher reactivity of the diamine than the monoamine was less related to the amounts of the NH₂ groups.

Furthermore, the structure and the thermal properties of these polyurea derivatives were characterized with XRD and DSC, respectively. XRD analyses showed that all the polyurea derivatives have a semi-crystalline structure except for the polyurea-IPDA, Fig. 4. The disordered H bonding formed in the polyurea-IPDA, which was confirmed by the FT-IR analysis as mentioned

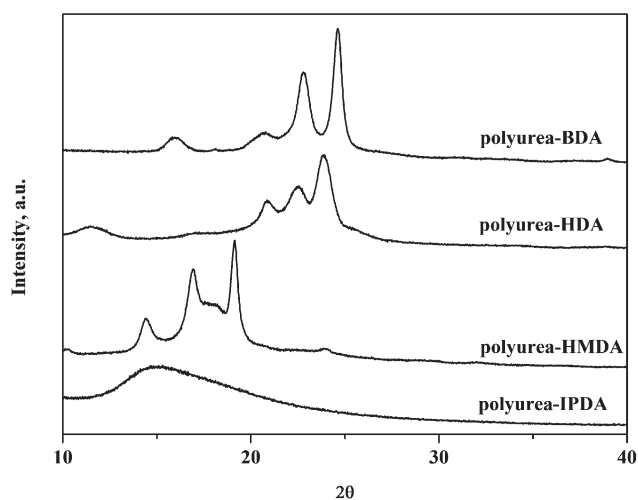


Fig. 4 XRD patterns of (a) polyurea-BDA (b) polyurea-HDA (c) polyurea-HMDA and (d) polyurea-IPDA.

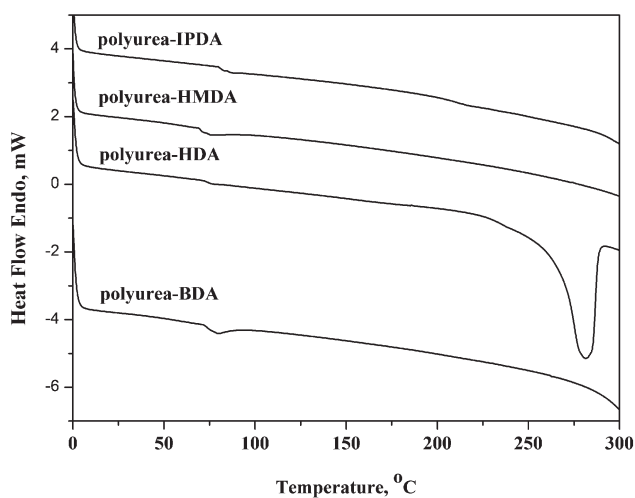


Fig. 5 DSC curves of (a) polyurea-BDA (b) polyurea-HDA (c) polyurea-HMDA and (d) polyurea-IPDA.

above, may be the major reason for the lower crystallinity in comparison with other polyurea derivatives. From the DSC curves of polyurea derivatives (Fig. 5), it can be seen that all the polyurea derivatives exhibited glass transition behavior during the heating process, but only the polyurea-HDA displayed a melting process (melting point: 278 °C). The glass transition temperature (T_g) of the polyurea-IPDA observed at 82 °C was higher than that of other polyurea derivatives ($T_g = 73, 74$ and 71 °C for polyurea-BDA, polyurea-HDA and polyurea-HMDA, respectively), which could be due to the lower flexibility and large hindrance of the cyclic structure with a side chain substituent.

Additionally, because the polyurea derivatives synthesized in this work were completely insoluble in conventional solvents, the measurement of the molecular weight and distributions become difficult *via* the traditional methods, such as end-group analyses, colligative methods, light scattering methods, viscometry, gel permeation chromatography or mass spectrometry.

Table 3 The results of BHDC synthesis from DBC and polyurea-HDA over different catalysts^a

Entry	Catalyst	Conversion (%)	Yield ^b (%)
1	None	1	Trace
2	NaOCH ₃	13	12
3	Bu ₂ SnO	75	73
4	MgO	26	25
5	3MgO–ZnO	53	52
6	MgO–ZnO	98	96
7	MgO–3ZnO	14	12
8	ZnO	12	10
9	Used MgO–ZnO	97	95
10	MgCO ₃ and ZnCO ₃	20	18

^a Reaction conditions: 5 mmol polyurea-HDA; 50 mmol DBC; 10 wt% catalyst (based on the mass of charged polyurea-HDA); 210 °C; 24 h. ^b Isolated based on the charged polyurea-HDA.

3.2 *N*-substituted carbamates syntheses from polyurea derivatives and dialkyl carbonates

A series of catalysts were screened for the dibutyl hexamethylenedicarbamate (BHDC) synthesis with DBC and polyurea-HDA, as shown in Table 3. In the blank test (entry 1), only a trace of BHDC was produced, suggesting that the catalyst was essential to such a reaction proceeding successfully. Previous studies showed that the basic catalysts, such as NaOCH₃ and Bu₂SnO, have good performance for the reaction of *N,N*-diphenyl urea and dialkyl carbonate, but showed poor to moderate catalytic activity for the production of BHDC and 13–75% polyurea-HDA conversions were achieved (entries 2–3). When a typical solid base, MgO, was used as a catalyst, it also showed poor catalytic activity (entry 4). When a zinc component was introduced into the magnesium oxide, the conversions of polyurea-HDA were greatly improved and increased first with increasing of zinc content, reaching its maximum 98% at a Mg/Zn molar ratio of 1 : 1, and then sharply decreased (entries 5–8). Furthermore, the catalytic activity of the MgO–ZnO catalyst has almost no changes after it was used for five runs (entry 9). Additionally, after the reaction, the catalyst was recovered through filtration, washing and calcination at 500 °C to remove the adsorbed organic materials, and it was found that 3 wt% of the catalyst was lost. The catalytic activity of the mixture of MgCO₃ and ZnCO₃ (6 mg, corresponding to 3 wt% of dissolved Mg²⁺ and Zn²⁺ from the originally charged MgO–ZnO catalyst during the reaction) was further tested (entry 10). The results showed that the mixture of MgCO₃ and ZnCO₃ gave low catalytic activity and 20% conversion of the polyurea-HDA was obtained, suggesting that the catalytic activity of the MgO–ZnO catalyst could be mainly derived from the heterogeneous MgO–ZnO catalyst, however, the phenomenon of homogeneous catalysis with Mg²⁺ and Zn²⁺ during the reaction could not be completely excluded.

By applying the optimized reaction conditions, the generality of the MgO–ZnO catalyst in *N*-substituted carbamates syntheses from different polyurea or urea derivatives and dialkyl carbonates was investigated (Table 4).

Table 4 Syntheses of *N*-substituted carbamates with different urea derivatives and dialkyl carbonates over MgO–ZnO catalyst^a

Entry	Urea derivatives	Dialkyl carbonate	Conversion (%)	Yield ^b (%)
1		DMC	97	65
2		DEC	98	79
3		DBC	98	96
4		DBC	96	95
5		DBC	95	93
6		DBC	99	98
7		DBC	98	97

^a Reaction conditions: 5 mmol urea derivatives; 50 mmol dialkyl carbonate; 10 wt% catalyst (based on the mass of charged urea derivatives); 210 °C; 24 h. ^b Isolated based on the charged urea derivatives.

Firstly, the impact of variation of the dialkyl carbonates on the polyurea-HDA reaction to form the corresponding *N*-substituted dicarbamates was tested, entries 1–3. When the dimethyl carbonate (DMC) and diethyl carbonate (DEC) were used as substrates, the conversions of polyurea-HDA were similar to that of DBC, but the selectivities of the corresponding dicarbamates were lower than those of DBC, which could be due to the formation of *N*-methylated or ethylated byproducts. A previous report⁴⁸ showed that the dialkyl carbonates are an attractive alternative as alkylating reagents for NH-containing compounds, and their alkylation ability under the same conditions is as follows: DMC > DEC > DBC. Thus, that there was no *N*-butylated product observed over DBC might be due to its lower reactivity for the alkylation. Then various polyurea or urea derivatives with different structures were further investigated (entries 4–7). Excellent yields of the corresponding *N*-substituted carbamates were obtained. The results also showed that the conversions of the polyurea derivatives based on diamines with a cyclic structure and the yields of the corresponding *N*-substituted dicarbamates were slightly lower than that of diamines with a linear chain structure and monoamines, which could be ascribed to the high steric hindrance of the cyclic structure.

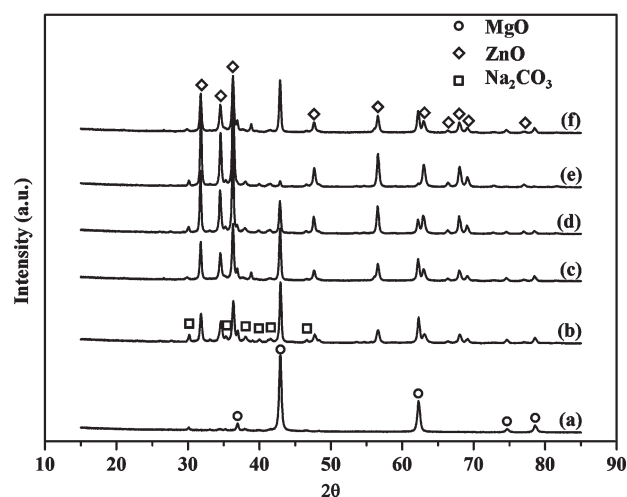
3.3 Results of the catalysts characterization

The physical properties of the catalysts are summarized in Table 5. Clearly, the BET surface area of the MgO–ZnO composite oxides sharply decreased when the zinc component was introduced into the magnesium oxide, and continuously decreased with increasing of the zinc content, which might be due to the fact that the BET surface area of the zinc oxide was much lower than that of magnesium oxide (entries 1–5).

Table 5 Physicochemical properties of the catalysts

Entry	Catalysts	S_{BET} (m ² g ⁻¹)	d_p (nm) ^a	v_p (cm ³ g ⁻¹) ^b	Total basic sites (μmol g ⁻¹)
1	MgO	29.1	26.3	0.21	69
2	3MgO–ZnO	10.5	25.6	0.06	23
3	MgO–ZnO	6.7	24.9	0.05	17
4	MgO–3ZnO	5.7	23.7	0.04	10
5	ZnO	5.5	11.7	0.02	8
6	Used MgO–ZnO	6.9	25.1	0.06	19

^a Average pore diameter. ^b Average pore volume.

**Fig. 6** XRD patterns of (a) MgO (b) 3MgO–ZnO (c) MgO–ZnO (d) MgO–3ZnO (e) ZnO and (f) used MgO–ZnO.

Meanwhile, the BET surface area of the used MgO–ZnO catalyst was almost unchanged after it was used five times (entry 6). The variation of the BET surface area of those MgO–ZnO composite oxides combined with their catalytic activities for the *N*-substituted carbamates syntheses from urea derivatives and dialkyl carbonates suggested that the BET surface area has little effect on the catalytic performance for such a catalytic system.

The XPS analyses of the fresh and used MgO–ZnO catalyst showed that the surface composition of the used MgO–ZnO catalyst was similar to that of fresh MgO–ZnO (Fig. S4†), suggesting that the catalyst surface was not changed after it was used five times.

XRD patterns of the MgO–ZnO composite oxides with different zinc content are shown in Fig. 6. For MgO and ZnO, the characteristic diffraction peaks of MgO and ZnO were observed and there were no other phases corresponding to the magnesium and zinc species. Moreover, the characteristic diffraction peaks of MgO and ZnO were observed for all the MgO–ZnO composite oxides, and the intensities of the ZnO characteristic diffraction peaks were enhanced and increased with increasing the zinc content. In addition to the characteristic peaks of MgO and ZnO, the characteristic peaks of the sodium carbonate also existed, which may be derived from the retained sodium carbonate during the catalyst preparation process. For used MgO–ZnO catalyst, its XRD patterns were found to be similar with that of the

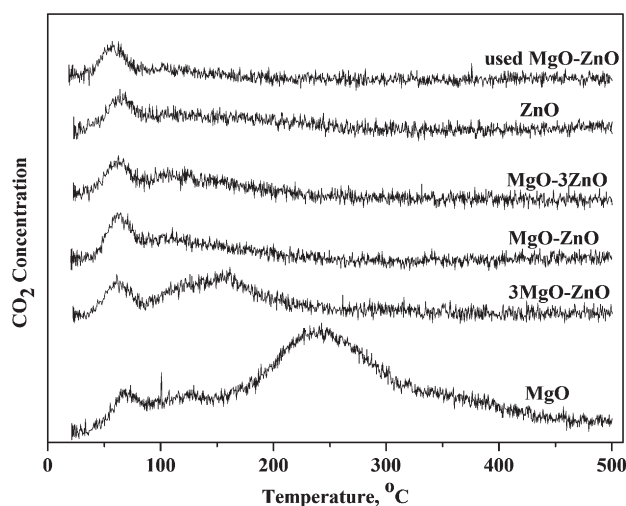


Fig. 7 TPD-CO₂ profiles of (a) MgO (b) 3MgO-ZnO (c) MgO-ZnO (d) MgO-3ZnO (e) ZnO and (f) used MgO-ZnO.

fresh MgO-ZnO catalyst, which suggested that the bulk structure of the MgO-ZnO was not changed after it was used five times.

The TPD-CO₂ results of MgO, 3MgO-ZnO, MgO-3ZnO, ZnO, fresh and used MgO-ZnO are shown in Fig. 7. Generally, a peak of CO₂ desorption appeared at about 78 °C and was observed over all the tested samples, this was derived from the weak strength basic sites. For the MgO sample, another broad peak centred at 250 °C was observed, which was attributed to medium strength basic sites. The broad peak of CO₂ desorption with medium strength basic sites was much reduced and finally disappeared when the zinc component was introduced and the zinc content was increased. In comparison with the fresh MgO-ZnO, the TPD-CO₂ profile of the used catalyst has almost no difference. From the quantitative results of TPD-CO₂ (Table 5), it can be seen that the total basic sites sharply decreased from 69 to 17 μmol g⁻¹ for pure MgO and MgO-ZnO, respectively, suggesting that the zinc component mainly affects the amount of the medium strength basic sites. Similar TPD-NH₃ characterization was also carried out over the MgO-ZnO composite oxide catalysts (not shown here), however, almost no NH₃ desorption peak on the TPD-NH₃ curves was observed, which suggested that these catalysts have weak or almost no acidities, but possessed weak basicities. According to the quantitative results of TPD-CO₂ and catalytic performance results of those catalysts, the conversions of polyurea-HDA were greatly increased with decreasing of the total basic sites, especially when the medium strength basic sites decreased, suggested that the medium basicity sites were unfavorable for the conversion of polyurea-HDA. With further decreasing of the total basic sites, mainly the weak basic sites, the conversions of the polyurea-HDA were sharply decreased, which could be ascribed to the much less basic sites. At this stage, much work is needed before clearly discerning the catalytic reaction mechanism, however, previous studies^{39,40} showed that the reaction between urea derivatives and dialkyl carbonates promoted with basic catalysts proceeded *via* a nucleophilic substitution mechanism, which indicated that the basic site of the catalyst acted as nucleophile reagents to activate the carbonyl of the dialkyl carbonates and polyurea derivatives. Based on

this reaction mechanism, the lower activities of the ZnO and MgO-3ZnO might be due to their lower amount of the basic sites and weak basicity, which were unfavorable for the nucleophilic attack on the carbonyl of the dialkyl carbonates and polyurea derivatives. But for MgO with medium basicity, which facilitated the nucleophilic attack on the carbonyl of the dialkyl carbonates and polyurea derivatives, such relatively strong interactions may lead to slower catalyst regeneration, resulting in lower activity of MgO. Therefore, incorporation of a zinc component into MgO may not only affect both the basicity strength and number of basic sites, but also affect the surface carbonation rate of the mixed oxide, which may result in higher catalytic activity. Therefore, the specific kinds and amounts of the basic sites might be the major reason for the high catalytic activity of MgO-ZnO.

4. Conclusions

In conclusion, an effective route for the syntheses of *N*-substituted carbamates from dialkyl carbonates and polyurea derivatives over MgO-ZnO catalyst was developed. The polyurea derivatives could be successfully synthesized from aliphatic diamines and CO₂ in the absence of any catalyst. Under the optimized reaction conditions, several important *N*-substituted carbamates were successfully synthesized with 93–98% isolated yields. The MgO-ZnO catalyst could be reused for several runs without deactivation. The characterization results of the catalysts suggested that the specific kinds and amounts of the basic sites might be the major reason for the highly catalytic activity of MgO-ZnO.

Acknowledgements

This work has been financially supported by the National Natural Science Foundation of China (No: 20773416).

Notes and references

- 1 A. J. Hunt, E. H. K. Sin, R. Marriott and J. H. Clark, *ChemSusChem*, 2010, **3**, 306–322.
- 2 P. Brannstein, D. Matt and D. Nobel, *Chem. Rev.*, 1988, **88**, 747–764.
- 3 T. Sakakura, J. C. Choi and H. Yasuda, *Chem. Rev.*, 2007, **107**, 2365–2387.
- 4 R. Nomura, Y. Hasegawa, M. Ishimoto, T. Toyosaki and H. Matsuda, *J. Org. Chem.*, 1992, **57**, 7339–7342.
- 5 H. Arakawa, *Stud. Surf. Sci. Catal.*, 1998, **114**, 19–462.
- 6 D. J. Darensbourg and M. W. Holtcamp, *Coord. Chem. Rev.*, 1996, **153**, 155–174.
- 7 F. Shi, Y. Deng, T. SiMa, J. Peng, Y. Gu and B. Qiao, *Angew. Chem., Int. Ed.*, 2003, **42**, 3257–3260.
- 8 K. Matsuda, *Med. Res. Rev.*, 1994, **14**, 271–301.
- 9 F. Bigi, R. Maggi and G. Sartori, *Green Chem.*, 2000, **2**, 140–148.
- 10 G. Bartolo, G. Salerno, R. Mancuso and M. Costa, *J. Org. Chem.*, 2004, **69**, 4741–4750.
- 11 S. Cenini and F. Ragaini, *Catalytic Reductive Carbonylation of Organic Nitro Compounds*, Kluwer Academic Publishers, 1997.
- 12 D. Niu, L. Zhang, L. Xiao, Y. Luo and J. Lu, *Appl. Organomet. Chem.*, 2007, **21**, 941–944.
- 13 J. Fournier, C. Bruneau, P. H. Dixneuf and S. Lécolier, *J. Org. Chem.*, 1991, **56**, 4456–4458.
- 14 T. Jiang, X. Ma, Y. Zhou, S. Liang, J. Zhang and B. Han, *Green Chem.*, 2008, **10**, 465–469.
- 15 B. M. Bhanage, S. Fujita, Y. Ikushima and M. Arai, *Green Chem.*, 2003, **5**, 340–342.

- 16 C. Wu, J. Wang, P. Chang, H. Cheng, Y. Yu, Z. Wu, D. Dong and F. Zhao, *Phys. Chem. Chem. Phys.*, 2012, **14**, 464–468.
- 17 P. Tundo and M. Selva, *Acc. Chem. Res.*, 2002, **35**, 706–716.
- 18 A. A. G. Shaikh and S. Sivaram, *Chem. Rev.*, 1996, **96**, 951–976.
- 19 S. Fukuoka, M. Kawamura, K. Komiyama, M. Tojo, H. Hachiya, K. Hasegawa, M. Aminaka, H. Okamoto, I. Fukawa and S. Konno, *Green Chem.*, 2003, **5**, 497–507.
- 20 P. Tundo, *Pure Appl. Chem.*, 2001, **73**, 1117–1124.
- 21 I. Vauthey, F. Valot, C. Gozzi, F. Fache and M. Lemaire, *Tetrahedron Lett.*, 2000, **41**, 6347–6350.
- 22 A. J. Wills, Y. K. Ghosh and S. Balasubramanian, *J. Org. Chem.*, 2002, **67**, 6646–6652.
- 23 J. P. Mayer, G. S. Lewis, M. J. Cuetius and J. Zhang, *Tetrahedron Lett.*, 1997, **38**, 8455–8448.
- 24 P. Uriz, M. Serra, P. Salagre, S. Castillon, C. Claver and E. Fernandez, *Tetrahedron Lett.*, 2002, **43**, 1673–1676.
- 25 A. M. Tares and J. Weygand, *Chem. Rev.*, 1996, **96**, 2035–2052.
- 26 S. Ozaki, *Chem. Rev.*, 1972, **72**, 457–496.
- 27 H. Eckert and B. Forster, *Angew. Chem., Int. Ed. Engl.*, 1987, **26**, 894–895.
- 28 L. Cotarca, P. Delogu, A. Nardelli and V. Sunjic, *Synthesis*, 1996, **5**, 553–576.
- 29 F. Ragaini, M. Gasperini and S. Cenini, *Adv. Synth. Catal.*, 2004, **346**, 63–71.
- 30 F. Paul, *Coord. Chem. Rev.*, 2000, **20**, 269–323.
- 31 B. Chen and S. S. C. Chuang, *Green Chem.*, 2003, **5**, 484–489.
- 32 F. Shi and Y. Deng, *J. Catal.*, 2002, **211**, 548–551.
- 33 Y. Ono, *Appl. Catal., A*, 1997, **155**, 133–166.
- 34 N. Lucas, A. P. Amrute, K. Palraj, G. V. Shanbhag, A. Vinu and S. B. Halligudi, *J. Mol. Catal. A: Chem.*, 2008, **295**, 29–33.
- 35 R. Juárez, A. Corma and H. García, *Top. Catal.*, 2009, **52**, 1688–1695.
- 36 J. Wang, Q. Li, W. Dong, M. Kang, X. Wang and S. Peng, *Appl. Catal., A*, 2004, **261**, 191–197.
- 37 S. P. Gupte, A. B. Shivarkar and R. V. Chaudhari, *Chem. Commun.*, 2001, 2620–2621.
- 38 A. B. Shivarkar, S. P. Gupte and R. V. Chaudhari, *J. Mol. Catal. A: Chem.*, 2004, **223**, 85–92.
- 39 J. Gao, H. Li, Y. Zhang and Y. Zhang, *Green Chem.*, 2007, **9**, 572–576.
- 40 J. Gao, H. Li, Y. Zhang and W. Fei, *Catal. Today*, 2009, **148**, 378–382.
- 41 X. Guo, J. Shang, J. Li, L. Wang, Y. Ma, F. Shi and Y. Deng, *Chin. J. Chem.*, 2010, **28**, 164–170.
- 42 M. Abila, J. C. Choi and T. Sakakura, *Chem. Commun.*, 2001, 2238–2239.
- 43 A. Ion, C. V. Dooslaer, V. Parvulescu, P. Jacobs and D. D. Vos, *Green Chem.*, 2008, **10**, 111–116.
- 44 M. Honda, S. Sonehara, H. Yasuda, Y. Nakagawa and K. Tomishige, *Green Chem.*, 2011, **13**, 3406–3413.
- 45 M. M. Coleman, M. Sobkowiak, G. J. Pehlert, P. C. Painter and T. Iqbal, *Macromol. Chem. Phys.*, 1997, **198**, 117–136.
- 46 J. Mattia and P. Painter, *Macromolecules*, 2007, **40**, 1546–1554.
- 47 A. Ion, V. Parvulescu, P. Jacobs and D. D. Vos, *Green Chem.*, 2007, **9**, 158–161.
- 48 I. A. Rivero, L. Guerrero, K. A. Espinoza, M. C. Meza and J. R. Rodríguez, *Molecules*, 2009, **14**, 1860–1868.